



Riverbank retreat analysis of the U-Tapao River, southern Thailand

Surat Semmad¹ · Tanit Chalermyanont^{1,2}

Received: 20 March 2017 / Accepted: 28 May 2018 / Published online: 14 June 2018
© Saudi Society for Geosciences 2018

Abstract

Riverbank retreat is a result of complex combinations of several processes, including subaerial processes, fluvial erosion, and bank failure. The objective of this study was to analyze riverbank retreat of six representative riverbanks along the U-Tapao River in southern Thailand using a process-based riverbank retreat model. Field and laboratory tests were conducted to determine index and engineering properties of the riverbank soil required in the modeling. In particular, the erodibility parameters of the riverbank soil were estimated using empirical formulae, measured in situ by performing a submerged jet test, and estimated from long-term bank retreat simulations using the Bank Stability and Toe Erosion Model (BSTEM) incorporated with a lumped adjustment factor. The observed bank retreat over the period from 2002 to 2016 obtained from analysis of aerial imagery was used to verify the validity of the riverbank retreat results. Good agreement with the observations was obtained from BSTEMs using adjusted erodibility parameters.

Keywords Critical shear stress · Erodibility coefficient · Riverbank retreat · BSTEM · Submerged jet test · The U-Tapao River

Introduction

Riverbank retreat is globally an important issue that affects infrastructure and stream-side properties, in-stream habitats, and water quality (Daly et al. 2015). Excessive sediment from riverbank erosion is among the most common surface water pollutants that degrade water quality and destroy aquatic habitats (ASCE 1998; Wynn and Mostaghimi 2006; Midgley et al. 2012). Moreover, many studies have demonstrated that riverbank erosion contributes a large portion of the sediment yield in a drainage system, which reduces the drainage capacity of the river and thereby causes flooding (e.g., Simon 1989; Grissinger et al. 1991). Thus, riverbank retreat involves the overall ecosystem of the river and causes huge economic losses with damage to natural resources (ASCE 1998).

Riverbank retreat is the integrated product of three main processes: subaerial processes, fluvial erosion, and bank failure (Hooke 1979; Lawler 1992; Lawler et al. 1997; Couper

and Maddock 2001; Rinaldi and Nardi 2013). Subaerial processes are climate-related phenomena that reduce soil strength, inducing direct erosion and making the bank more susceptible to fluvial erosion by, for example, desiccation cracking (Thorne 1982). Fluvial erosion is the removal of bank material by the action of the river's hydraulic forces (Rinaldi and Nardi 2013), while the collapse of riverbanks due to slope instability is referred to as bank failure (Lawler 1995). Riverbank retreat is a cyclic process, initiated by the fluvial erosion of the river bed and/or toe, which creates a geotechnically unstable riverbank. This instability results in riverbank failure and deposition of failed materials at the bank toe. Subsequent floods remove that failed materials and the bank retreat cycle is repeated until the channel widens enough to reduce the boundary shear stresses to non-erosive levels (Thorne 1982).

The erosion rate of cohesive riverbank is commonly predicted using the excess shear stress equation (Partheniades 1965; Hanson 1990a, 1990b):

$$\varepsilon = k_d(\tau_o - \tau_c)^a \quad (1)$$

where ε is the rate of erosion (m/s), k_d is the erodibility coefficient ($\text{m}^3/\text{N}\cdot\text{s}$), τ_o is the developed boundary shear stress (Pa), τ_c is the critical shear stress (Pa), and a is an empirical exponent, often in practice assumed to be unity (Hanson

✉ Tanit Chalermyanont
tanit.c@psu.ac.th

¹ Department of Civil Engineering, Prince of Songkla University, Hat Yai, Songkhla 90112, Thailand

² Southern Natural Disaster Research Center, Prince of Songkla University, Hat Yai, Songkhla 90112, Thailand

1990a, 1990b; Hanson and Cook 2004). The riverbank erosion is initiated by non-negative excess shear stress ($\tau_o - \tau_c$). Once the erosion is initiated, k_d defines the rate at which particles are detached from the riverbank (Daly et al. 2013).

In the excess shear stress equation, while τ_o is simply related to the flow rate of water ($\tau_o = \gamma_w RS$, where γ_w is the unit weight of water, R is the local hydraulic radius calculated from the water depth, and S is the channel slope (Daly et al. 2015)), the soil erodibility parameters (τ_c and k_d) are difficult to quantify (Grissinger 1982). There are many approaches for determining the erodibility parameters. Several studies have derived τ_c and k_d for cohesive soils using various techniques such as flume tests (Hanson and Cook 1997), a laboratory hole erosion test (Briaud et al. 2001; Wan and Fell 2004), and a submerged jet test (Hanson and Cook 1997; Clark and Wynn 2007). Based on such experimental results, many studies have proposed simpler approaches to estimate τ_c from other soil properties: from clay content and liquid limit (Smerdon and Beasley 1961), silt-clay content (Julian and Torres 2006), and from unconfined compressive strength (Kamphius and Hell 1983). Once τ_c is determined, k_d can be estimated from empirical formulae (e.g., Hanson and Simon 2001; Wynn 2004; Simon et al. 2011).

Alternatively, in situ measurement of the erodibility parameters can be done using the submerged jet device developed by Hanson (1990b). The jet test is preferred over the flume tests because it can be conducted directly on the intact riverbank material without sampling and sample preparation that would disturb the soil structure, as they do in the flume tests. Determination of τ_c and k_d using the jet test results (i.e., jet pressure and scour depth created) has been proposed by many researchers, such as Hanson and Cook (1997, 2004) and Daly et al. (2013). A detailed description of the jet device and the testing methodology is presented elsewhere (Hanson and Cook 1997; Hanson and Simon 2001; Al-Madhhachi et al. 2013).

Recently, Daly et al. (2015) evaluated the erodibility parameters of the Barren Fork Creek in eastern Oklahoma, USA, by calibration of a process-based riverbank retreat model. Streambank geography, bank soil properties, stream hydrograph, and initial erodibility parameters obtained from the jet test were used as inputs to the process-based riverbank erosion model (i.e., the Bank Stability and Toe Erosion Model, BSTEM), developed by the National Sedimentation Laboratory in Oxford, MS. The computed streambank was compared with the actual streambank retreat obtained from aerial imagery. The initial erodibility parameters were then adjusted until the computed streambank retreat was similar to the observed streambank retreat. The erodibility parameters obtained in this manner accounted for fluvial erosion and bank failure, along with several other field factors such as curvature-driven and turbulence-driven secondary flows and

spatial and temporal changes of bank materials due to cyclical wetting and drying.

As a part of the U-Tapao River erosion study and protection project, the objective of this study was to analyze riverbank retreat of six representative composite riverbanks along the U-Tapao River in southern Thailand. The field survey was conducted to determine geometry of the riverbanks. In situ and laboratory measurements were performed to assess the riverbank soil geotechnical and erodibility parameters. Aerial imagery analysis was conducted to determine the actual bank retreats. The Bank Stability and Toe Erosion Model (BSTEM) was used to compute the riverbank retreats. The computed results were verified and validated using measured riverbank retreats from aerial imagery analysis.

Description of the study area

The study area is located in the U-Tapao River watershed, in the southern part of Thailand (Fig. 1). The U-Tapao River watershed covers 2392 km² from the southern Thai-Malaysian border to the Songkhla Lake. This is the most important watershed of southern Thailand and is home to over 700,000 residents. Hat Yai city, the main city in the watershed, is a local center of economy, industry, and tourism in this region. The U-Tapao River, the main river in the watershed, is about 112 km long. It originates in the southern mountainous areas, flows northward through the center of the watershed, and drains into the Songkhla Lake. The average annual rainfall of the watershed is about 1524 mm due to the tropical monsoon climate in this region. Heavy rains in the months from October to December often cause great erosion and frequent failures of the riverbanks.

U-Tapao riverbanks along the midstream area of the watershed are reportedly experiencing high bank retreat problems and were selected as the study area. In this area, the U-Tapao River is about 20 to 40 m wide and 5 to 10 m deep. A picture of the U-Tapao River composite bank in the study area (Fig. 2) shows a typically steep bank face. The typical composite riverbanks in the study area consist mainly of two layers. The top layer (hereafter called “upper bank”) is low plasticity cohesive soil with thickness ranging from about 1.0 to 1.5 m. The underlying layer (hereafter called “lower bank”) is either cohesive or granular soil, which normally ranges in thickness from about 3.0 to 6.0 m. Field observation indicates toe erosion at the lower banks continuously leads to bank failure and retreat. In this study, six sites were selected at locations along the midstream area of the U-Tapao River and are designated as UT1 to UT6, as shown in Fig. 1 and Table 1. The distance from UT1 to UT6 is about 14 km. Pictures of the

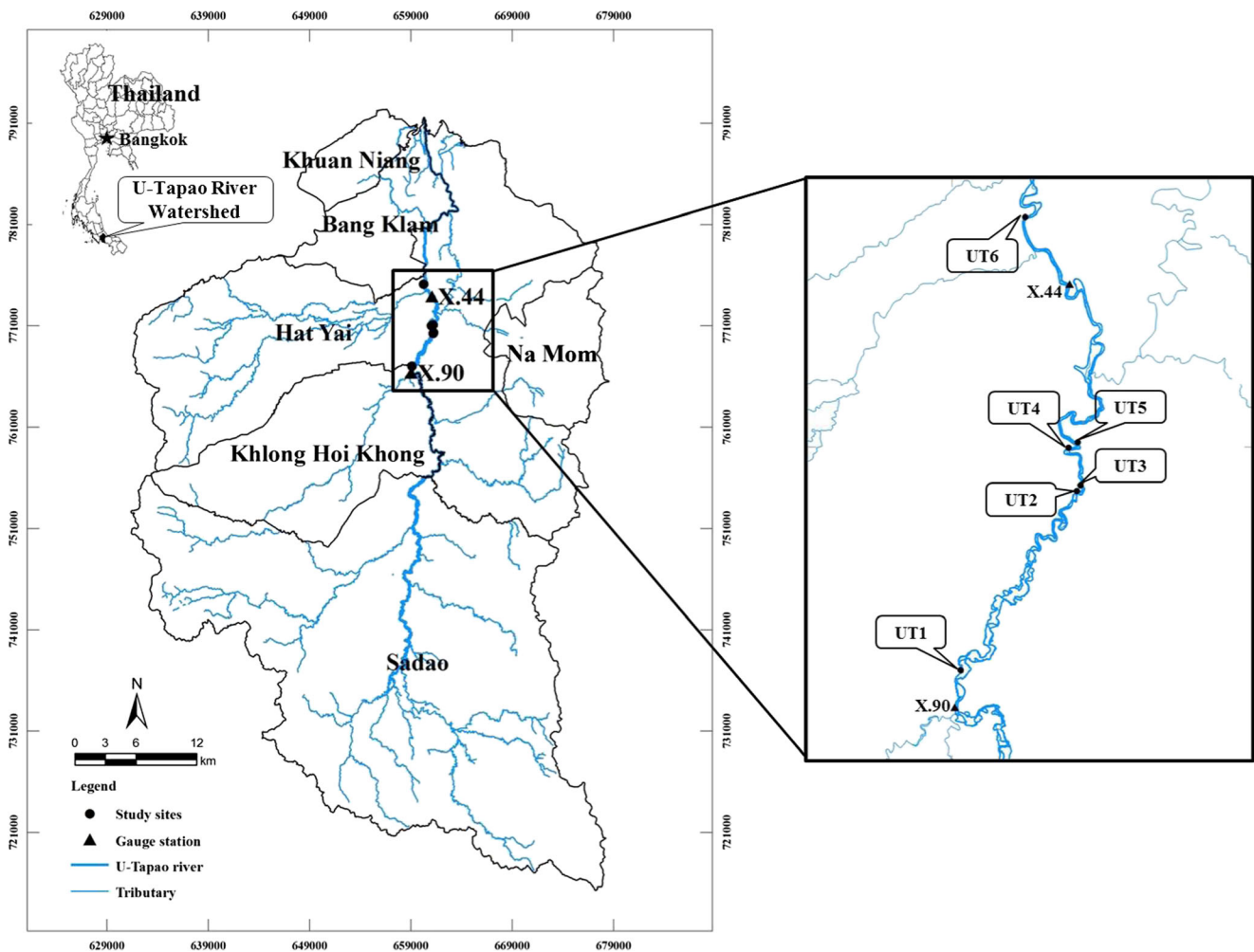


Fig. 1 U-Tapao River watershed and the study site locations

U-Tapao River bank sites are shown in Fig. 3. Around these sites, the typical land use is as para rubber plantations that have bank retreat problems according to local

authorities and land owners. At each site, a representative cross section and a detailed bank stratigraphy were prepared using field survey data.

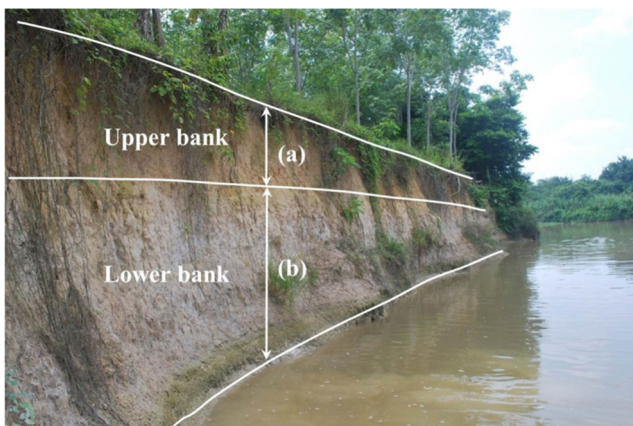


Fig. 2 An U-Tapao River composite bank showing the typical layers. Upper bank with low plasticity cohesive soil (a) and lower bank with cohesive or granular soil (b)

Background

Empirical relationships for determining erodibility parameters

There are several approaches to determine soil erodibility parameters. The parameters can be simply estimated from empirical relationships using soil index properties, as proposed by several researchers. Estimates of τ_c can be obtained from empirical equations using plasticity index, dispersion ratio, mean particle size, and percent clay (Smerdon and Beasley 1961), silt-clay content (Julian and Torres 2006), unconfined compressive and vane shear strength (Kamphius and Hell 1983), and dispersion ratio, activity, and soil pH (Thoman and Niezgodna 2008). Based

Table 1 Soil properties at the six study sites

Site	Latitude, longitude (m)	Bank layer	Depth from bank top (m)	D_{50} (mm)	P_c (%)	PI (%)	SC (%)	γ (kN/m ³)	USCS	Shear strength parameters	
										ϕ' (°)	c' (kPa)
UT1	767,023, 659,154	Upper	0.00–1.30	0.047	17.13	6.90	57.91	16.90	CL	30.17	8.24
		Lower	1.31–4.60	0.070	13.01	5.38	47.96	18.23	CL	27.55	9.75
UT2	770,216, 661,222	Upper	0.00–1.50	0.007	35.00	14.70	86.00	18.67	CL	27.38	12.48
		Lower	1.51–4.34	0.250	1.39	NP	10.77	20.11	SM	33.74	1.26
UT3	770,317, 661,286	Upper	0.00–1.40	0.010	25.90	11.54	72.00	18.02	ML	27.17	9.56
		Lower	1.41–4.49	0.103	6.25	NP	41.63	17.98	ML	28.38	5.07
UT4	770,986, 661,074	Upper	0.00–1.50	0.035	17.62	9.33	63.39	17.86	CL	22.61	17.05
		Lower	1.51–7.78	0.236	3.24	NP	13.63	17.63	SM	28.94	2.01
UT5	771,082, 661,237	Upper	0.00–1.00	0.065	11.28	7.54	48.90	18.16	CL	24.31	3.12
		Lower	1.01–5.57	0.001	57.88	17.23	88.00	19.87	CL	23.97	18.27
UT6	775,103, 660,303	Upper	0.00–1.50	0.065	6.93	7.30	49.21	17.23	CL	31.30	3.19
		Lower	1.51–5.16	0.001	61.40	35.12	94.00	18.31	CH	25.52	17.78

D_{50} , median particle size of soil; P_c , percentage of clay content; PI , plasticity index; SC , percentage of silt-clay content; γ , bulk unit weight; $USCS$, Unified Soil Classification System; ϕ' , effective internal friction angle; c' , effective cohesion

on flume testing results, Smerdon and Beasley (1961) developed empirical relationships of τ_c to various soil index properties, as shown in Eqs. 2–4.

$$\tau_c = 3.54 \times 10^{-28.1D_{50}} \quad (2)$$

$$\tau_c = 0.493 \times 10^{0.0182P_c} \quad (3)$$

$$\tau_c = 0.16(PI)^{0.84} \quad (4)$$

where τ_c is the critical shear stress (Pa), D_{50} is the median particle size of soil (mm), P_c is the percentage of clay content (i.e., content of soil particles less than 0.002 mm in size), and PI is the soil plasticity index.

Julian and Torres (2006) established an empirical equation to estimate τ_c from the percentage of silt-clay (SC):

$$\tau_c = 0.1 + 0.1779(SC) + 0.0028(SC)^2 - 2.34 \times 10^{-5} \times (SC)^3 \quad (5)$$

Unlike τ_c , empirical estimates of k_d from the soil properties are not available (Hanson and Temple 2002). However, k_d can be given empirical estimates from known τ_c . Such empirical relations between k_d and τ_c have been developed based on submerged jet test results and are often power laws (Hanson and Simon 2001; Wynn 2004; Thoman and Niezgodna 2008). Using the Blaisdell solution (Blaisdell et al. 1981), Simon et al. (2010) concluded from jet test results that k_d is related to τ_c as shown in Eq. 6. Daly et al. (2013) developed a scour depth

solution method to fit the jet test results and proposed the relationship in Eq. 7.

$$k_d = 1.62\tau_c^{-0.838} \quad (6)$$

$$k_d = 157\tau_c^{-1.620} \quad (7)$$

where k_d is the erodibility coefficient (cm³/N.s) and τ_c is the critical shear stress (Pa). The discrepancy between the various empirical models indicates that, while the type of model might have wide applicability, each model fit is restricted to a specific context of soil samples.

Submerged jet test

For cohesive soils, the soil erodibility parameters can be experimentally determined using an in situ submerged jet device. Designed by Hanson (1990b), the device distributes a circular jet through the nozzle at a uniform velocity, to produce shear stresses in the bank material. Consequently, the scours or the eroded depths generated are measured, and their time profiles are used to determine the erodibility parameters. Hanson and Cook (1997) developed an analytical procedure to estimate τ_c by fitting a hyperbolic logarithm equation proposed by Blaisdell et al. (1981) to the scour depth vs time data, while k_d was estimated by fitting the scour data to the excess shear stress equation (Eq. 1). Daly et al. (2013) stated that the conventional Blaisdell solution method is too conservative, so they developed an alternative approach, the so-called scour depth solution method.

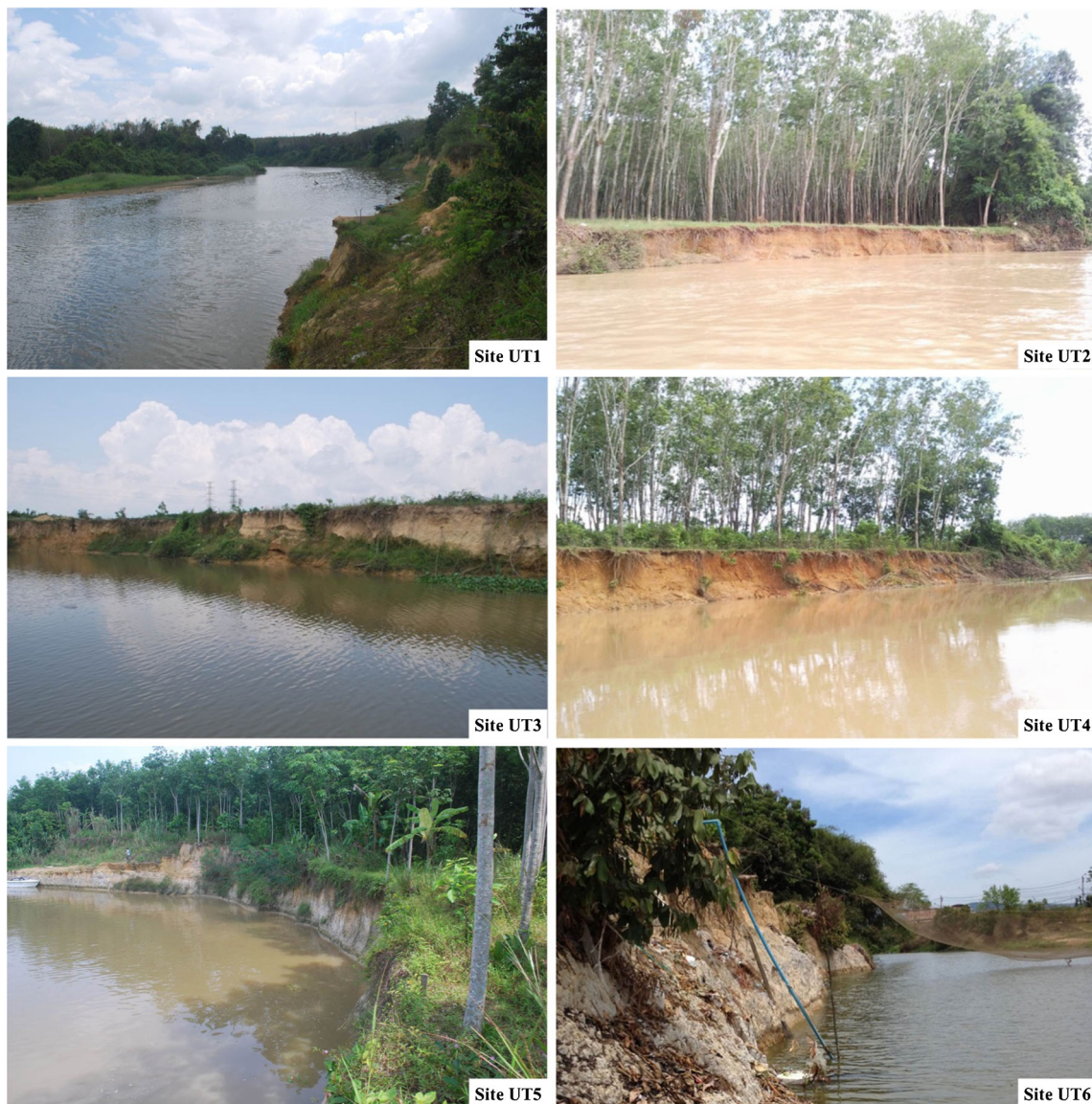


Fig. 3 Pictures of U-Tapao River banks showing composite and cohesive riverbanks with steep bank faces

The jet test device has been used numerous times to determine the erodibility of cohesive soils (Hanson et al. 1999; Langendoen et al. 2000; Hanson and Simon 2001; Semmens and Osterkamp 2001; Simon and Thomas 2002; Thoman and Niezgod 2008; Karmaker and Dutta 2011). Results from most of these studies indicate large variations in τ_c and k_d . After conducting 83 jet tests on stream beds of highly erodible loess in the Midwest of USA, Hanson and Simon (2001) found that τ_c ranges from 0.0 to 400 Pa and k_d ranges from 0.001 to 3.75 cm³/N.s. Thoman and Niezgod (2008) investigated the channel stability of the Power River Basin in Wyoming. They determined erodibility parameters of the cohesive banks using jet tests and found the range for 0.11 to 15.35 Pa for τ_c and from 0.27 to 2.38 cm³/N.s for k_d . Karmaker and Dutta (2011) studied the erodibility parameters of many sites along the Brahmaputra in India and reported the

ranges from 0.1 to 100 Pa for τ_c and from 0.519 to 11.28 cm³/N.s for k_d .

Process-based riverbank retreat model

A process-based riverbank retreat model has been used to compute the bank retreat and to study factors affecting bank stability and erosion (Wilson et al. 2007; Cancienne et al. 2008; Midgley et al. 2012; Daly et al. 2015). It consists of two main processes which are the bank erosion and the bank failure. The bank erosion includes both bank and bank toe erosions by hydrological processes (e.g., rainfall, river hydrograph, groundwater oscillations) that lead to bank profile changes over time (Rinaldi and Nardi 2013). The bank failure process involves reduction of the resisting forces in the bank soil mass by several factors, such as toe erosion

and shear strength decrease due to wetting of soil, until the resisting forces are exceeded by the bank self-weight. The most common process-based riverbank retreat model is the Bank Stability and Toe Erosion Model (BSTEM) developed by the National Sedimentation Laboratory in Oxford, MS, USA (Simon et al. 2000). The current version of BSTEM (Dynamic Version 5.4) has bank stability and toe erosion modules, and the capacity to model a continuous hydrograph by sequentially applying the various model components for a stream depth defined by the hydrograph, redrawing the bank profile, and then moving to the next step of hydrograph (Daly et al. 2015).

Daly et al. (2015) used BSTEM to determine erodibility parameters of composite streambanks by calibrating the parameters to fit two temporal streambank retreat data sets from aerial imagery. They stated that spatial and temporal changes occur in the fluvial resistance of bank materials due to wetting/drying cycles. In addition, the deeper and faster flows at the outsides of river bends exert elevated shear stresses on the streambank. Therefore, τ_c and k_d can change considerably over time due to the wetting/drying cycles and the subaerial processes. They suggested that a “lumped” adjustment factor (α , dimensionless) should be used to modify Eq. 1, to account for the simplified hydraulics in BSTEM as well as for potential changes in erodibility, as shown in Eq. 8. This adjustment factor has been utilized in long-term analyses of repeating bank retreats in several prior studies (Langeodoen and Simon 2008; Lai et al. 2012; Nardi et al. 2013; Daly et al. 2015).

$$\varepsilon = k_d(\alpha\tau_o - \tau_c) = \alpha k_d \left(\tau_o - \frac{\tau_c}{\alpha} \right) \quad (8)$$

where ε is the rate of erosion (m/s), k_d is the erodibility coefficient ($\text{m}^3/\text{N}\cdot\text{s}$), τ_o is the developed boundary shear stress (Pa), τ_c is the critical shear stress (Pa), and α is a “lumped” adjustment factor.

Methodology

In situ measurements with a submerged jet test device

In situ measurements of soil erodibility parameters were performed using a submerged jet test device during January to February 2015. The jet test device and the testing procedures complied with ASTM D5852. A total of 24 jet test runs were conducted at the six selected sites described previously. Duplicate jet test runs were conducted on both upper and lower banks at each site (four tests per site). Each test was conducted for 50 min, with scour depth and pressure differential readings taken at 5-min intervals. The τ_c and k_d were

estimated from the scour and shear stress data obtained, using the scour depth solution method developed by Daly et al. (2013).

Soil testing

At each site, both disturbed and undisturbed soil samples were collected. The disturbed samples were air-dried prior to conducting index property tests. The median particle diameter (D_{50}) and the mass fraction passing sieve no. 200 (i.e., sieve size of $0.75 \mu\text{m}$) were determined according to the soil particle size distribution test (ASTM D6913). Plastic limit, liquid limit, and plasticity index of each soil sample were determined following ASTM D4318. Hydrometer analysis (ASTM D422) was conducted to determine the silt-clay content (SC). For the undisturbed samples, the multi-stage direct shear (MSDS) test was performed according to ASTM D3080 to determine the shear strength parameters, namely the effective cohesion (c') and the effective internal friction angle (ϕ').

Aerial imagery analysis

Aerial imagery analysis was conducted to determine the actual bank retreat over time. Aerial images with 0.5-m resolution representing the years 2002, 2010, and 2016 (Fig. 4) were obtained from the Royal Thai Survey Department for the analysis. All the aerial images were geo-referenced with the World Geodetic System 1984 (WGS-84) using ArcGIS10. For each site, the bank edges were digitized along the field-determined reach length. Retreat was determined to have occurred when the digitized bank in the next image appeared to be farther away from the river centerline of year 2002. For example, the 2002 river centerline shown as a light line in Fig. 4 acted



Fig. 4 Aerial photograph of U-Tapao River for bank retreat determination by analysis of aerial imagery

as a reference line, and three digitized bank locations were then overlaid onto the 2016 image. A series of transects were created from the centerline to the bank locations, and the corresponding transect lengths were measured. The bank retreat at each transect was computed by subtracting the current transect length from the previous one. A single bank retreat number for each site was computed by averaging the bank retreats across all transects along the reach length. In this study, the bank retreat for 2010, designated by R_{2010} (m) was defined as the bank retreat from comparing years 2002 and 2010. Correspondingly, R_{2016} (m) denotes the bank retreat from comparing 2010 and 2016. The total bank retreat (R_T) denotes the sum of R_{2010} and R_{2016} .

Riverbank retreat analysis

In this study, a bank retreat analysis for the U-Tapao River was conducted using BSTEM (Dynamic Version 5.4) according to the procedure developed by Daly et al. (2015). The BSTEM input data include river cross section, shear strength parameters, erodibility parameters, and river hydrograph. A representative cross section obtained from field survey was used as the bank geometry. The shear strength parameters (c and ϕ) were obtained from the multi-stage direct shear test described previously. The τ_c and k_d were obtained from the jet tests and were used as initial erodibility parameters. River hydrographs and rating curves for the period from 2002 to 2016, by two nearby available stations (X44 and X90 stations in Fig. 1) of the Royal irrigation department, provided the hydraulic loading at the bank faces. A specific hydrograph for each site was

generated via back water curve analysis using boundary conditions such as upstream water discharge, downstream water level, and downstream bed level from both control stations. All generated hydrographs had the same pattern. A representative hydrograph from site UT6 is shown in Fig. 5.

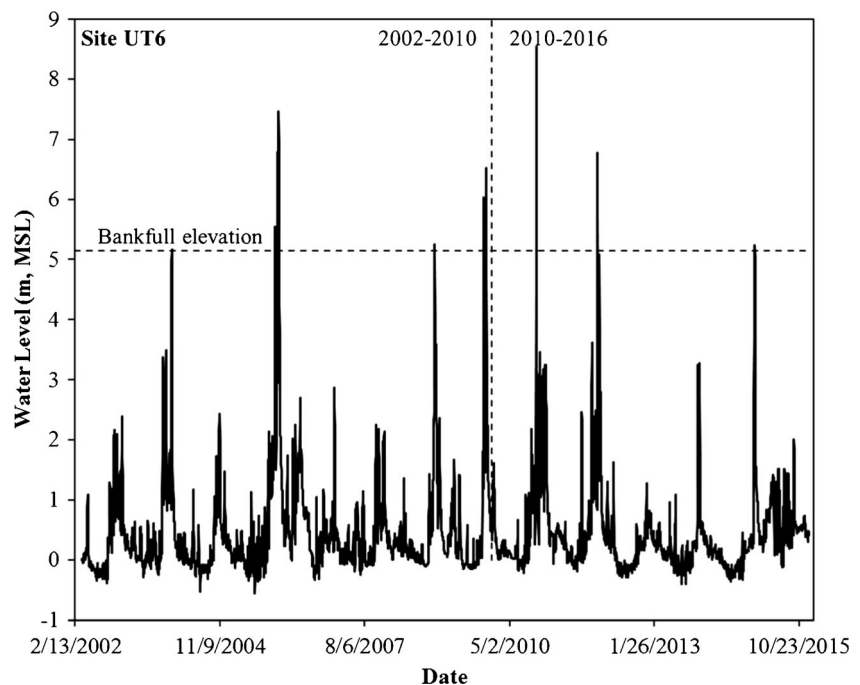
Bank retreat results from the BSTEM runs (BSTEM R_{2010}) were compared with the aerial R_{2010} obtained from aerial imagery analysis. When BSTEM R_{2010} did not equal the aerial R_{2010} , this indicated that the initially used erodibility parameters did not represent the field conditions hydrologically and geotechnically. The initial τ_c and k_d were then adjusted using the lumped calibration factor (α) described in Eq. 8, and BSTEM R_{2010} was recomputed. This was iterated until the difference between BSTEM and aerial R_{2010} was less than 0.5 m (which is the resolution of the aerial images) and the lumped τ_c and k_d were obtained. To verify that these lumped τ_c and k_d values were good for modeling the bank retreat, another set of BSTEM runs was conducted using the 2010 to 2016 hydrographs, and the corresponding BSTEM R_{2016} values were computed. The BSTEM R_{2016} model predictions were then compared to observed R_{2016} from aerial imagery analysis, to validate the models using lumped τ_c and k_d values.

Results and discussion

Soil testing results

The laboratory test results are shown in Table 1. Thickness of the upper bank ranged from 1.0 to 1.5 m. The upper bank soil

Fig. 5 A hydrograph of the site UT6 used in BSTEM analysis



was classified as either low plasticity silt (ML) or as low plasticity clay (CL), with D_{50} values from 0.007 to 0.065 mm, SC values from 48.9 to 86.0%, P_c values from 6.93 to 35.0%, and PI values from 6.90 to 14.7%. Despite being classified as silty or clayey soils, these fine-grained soils with low plasticity exhibit properties between cohesive and non-cohesive soils, and the properties are not exclusively dependent on particle mass and interparticle electrochemical interactions (Grissiniger et al. 1981). Regarding the lower banks, as shown in Table 1, their thickness varied from 2.8 to 6.2 m. Both fine- and coarse-grained soil types were found. They fell into a wide range of soil types, including silty sand (SM), low plasticity silt (ML), low plasticity clay (CL), and high plasticity clay (CH). Fine-grained soil (i.e., ML, CL, and CH) was found in the sites UT1, UT3, UT5, and UT6, while coarse-grained soil (i.e., SM) was found in the sites UT2 and UT4. Shear strength parameters of the upper and lower bank soil (Table 1) were obtained using multi-stage direct shear tests. Effective cohesion (c') ranged from 3.12 to 17.05 (from 1.26 to 18.27) kPa and the effective internal friction angle (ϕ') ranged from 22.61 to 31.30 (from 23.97 to 33.74) ° for the upper (lower) bank soils.

Erodibility parameters from jet tests and empirical formulae

The jet test results are presented in Table 2. It was found that τ_c of the riverbanks at the selected sites varied in a comparatively narrow range, by about an order of magnitude. The data in

Table 2 indicate that the upper bank soil was slightly more erosion resistant than the lower bank soil. The τ_c ranged from 7.12 to 20.93 Pa with a median of 10.99 Pa in the upper bank, while it ranged from 1.43 to 16.88 Pa with a median of 8.525 Pa in the lower bank. The k_d value ranged from 1.74 to 14.29 cm³/N.s with a median of 3.76 cm³/N.s. in the upper and from 3.67 to 19.55 cm³/N.s with a median of 9.67 cm³/N.s in the lower bank.

The τ_c and k_d data in Table 2 were plotted to assess the relationship of τ_c and k_d (Fig. 6). Additionally, erodibility categories as proposed by Hanson and Simon (2001) are also shown in Fig. 6. It was found that the riverbank soil mostly fell in the category “very erodible.” Only the CL soil from sites UT4 and UT6 had sufficient erosion resistance to be considered “erodible.” As demonstrated by Simon et al. (2010) in Eq. 6 and Daly et al. (2013) in Eq. 7, τ_c and k_d are inversely related and tend to be related by a power law. In this current study, the relationship of τ_c and k_d was fit by the solid line in Fig. 6:

$$k_d = 19.54\tau_c^{-0.547} \quad (9)$$

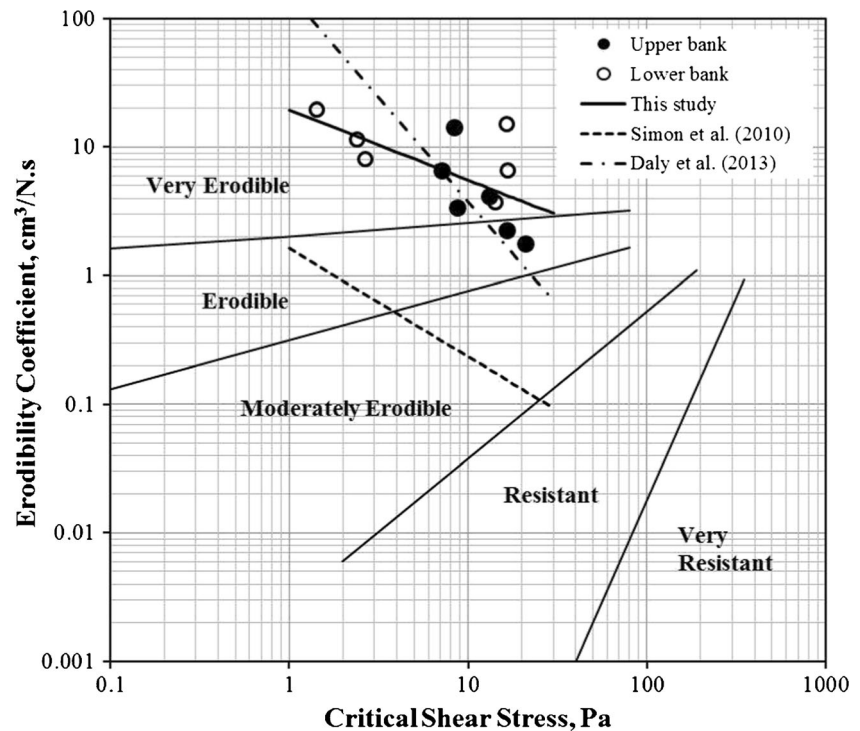
where k_d is the erodibility coefficient (cm³/N.s) and τ_c is the critical shear stress (Pa). It is also seen in Fig. 6 that the relationship between τ_c and k_d obtained in this study has similar trend as that in Daly et al. (2013), whereas the fit in Simon et al. (2010) tends to underestimate the k_d in our data. This may be due to the fact that Simon et al. (2010) used the Blaisdell solution method to estimate τ_c and k_d , while Daly et al. (2013)

Table 2 Jet test results and estimates of erodibility parameters using empirical formulae

Site	Bank layer	Computed τ_c (Pa)				JET test		Computed k_d^* (cm ³ /N.s)		
		D_{50} (Eq. 2)	P_c (Eq. 3)	PI (Eq. 4)	SC (Eq. 5)	τ_c (Pa)	k_d (m ³ /N.s)	Simon et al. (2010, Eq. 6)	Daly et al. (2013, Eq. 7)	This study (Eq. 9)
UT1	Upper	0.17	1.01	0.81	15.25	13.18	4.13	0.17	1.90	4.40
	Lower	0.04	0.85	0.66	12.49	14.37	3.67	0.20	2.63	4.91
UT2	Upper	2.25	2.14	1.53	21.22	20.93	1.74	0.13	1.11	3.67
	Lower	–	0.52	–	2.31	1.43	19.55	0.80	40.41	12.36
UT3	Upper	1.85	1.46	1.25	18.69	7.12	6.48	0.14	1.37	3.94
	Lower	–	0.64	–	10.67	2.41	11.36	0.22	3.39	5.35
UT4	Upper	0.37	1.03	1.04	16.67	16.47	2.23	0.15	1.65	4.19
	Lower	–	0.56	–	2.99	2.68	7.98	0.65	26.69	10.74
UT5	Upper	0.05	0.79	0.87	12.76	8.80	3.39	0.19	2.54	4.85
	Lower	3.23	5.57	1.75	21.49	16.88	6.55	0.12	1.09	3.65
UT6	Upper	0.05	0.66	0.85	12.85	8.41	14.29	0.19	2.51	4.84
	Lower	3.30	6.46	3.18	22.13	16.56	15.07	0.12	1.04	3.59
Median		0.37	0.93	1.04	14.05	10.99	6.51	0.18	2.21	4.62
Max		3.30	6.46	3.18	22.13	20.93	19.55	0.80	40.41	12.36
Min		0.04	0.52	0.66	2.31	1.43	1.74	0.12	1.04	3.59

* k_d computed using τ_c obtained from Eq. 5

Fig. 6 Relationship of the critical shear stress and the erodibility coefficient, as obtained from the jet tests



and the present study use the scour depth solution method. In the Blaisdell solution, the measured scour time data may give unreliable estimates of both τ_c and k_d (Simon et al. 2010).

The estimated erodibility parameters are tabulated in Table 2. The τ_c was measured in situ with the jet test and estimated using the median particle size (D_{50}) and Eq. 2, using percentage of clay content (P_c) and Eq. 3, and using plasticity index (PI) and Eq. 4. The median values were 10.99, 0.37, 0.93, and 1.04 Pa, in the same order. The τ_c values estimated using D_{50} , P_c , and PI were as much as two orders of magnitude below the experimental τ_c from the jet test. This indicates that estimates of τ_c from the formula by Smerdon and Beasley (1961) can be very poor. Estimates using the silt-clay content (SC , Eq. 5) following Julian and Torres (2006) were better. Comparing the estimates for an individual site and for its upper and lower banks, the measured jet test τ_c values were relatively similar to those estimated from SC . For example, for UT4 (Table 2), the τ_c from jet test for the upper (lower) bank was 16.47 (2.68) Pa, while the corresponding estimate was 16.67 (2.99) Pa. Also, Karmaker and Dutta (2011) reported that their best estimates of τ_c were based on SC . They stated that the submerged jet test method provides a better estimate of the τ_c under field conditions, while the SC -based estimate may be used as an alternative method of estimation.

The k_d from jet tests and corresponding estimates are given in Table 2. Estimates of k_d were based on Eq. 6 (Simon et al. 2010), Eq. 7 (Daly et al. 2013), and Eq. 9 (this study), using only the estimates of τ_c based on SC content (Eq. 5). The median k_d values were 6.51, 0.18, 2.21, and 4.62 $\text{cm}^3/\text{N.s}$, from the jet test and from Eqs. 6, 7, and 9, in this order. The

data in Table 2 indicate that Eq. 9 provided the best estimates of k_d , while Eq. 7 was better than Eq. 6. As previously mentioned, use of the scour depth solution method in Eqs. 7 and 9 resulted in better estimates of k_d than the Blaisdell solution method with Eq. 6.

Aerial imagery analysis results

The results from analysis of aerial images representing 2002, 2010, and 2016 (Table 3) indicate that bank retreat took place at every site. The R_{2010} (bank retreat from 2002 to 2010) ranged from 3.04 m (site UT6) to 11.76 m (site UT5) with an average retreat of 8.33 m, while the R_{2016} (bank retreat from 2010 to 2016) ranged from 1.87 m (site UT1) to 20.06 m (site UT5) with an average of 8.88 m. The R_T (bank retreat from 2002 to 2016) ranged from 7.52 m (site UT6) to 31.83 m (site UT5) with an average of 17.21 m. The retreats observed for the sites UT2 to UT4 were closely similar (Table 3). This is reasonable as these sites are located close to each other (about 1.4 km apart), so their soil properties and hydraulic loadings are expected to not differ by much.

The least 7.52-m R_T was found at the site UT6, which might be caused by several factors. The lower bank soil of this site was high plasticity clay (CH) with high effective cohesion, resulting in low bank failure potential and correspondingly low bank retreat. In addition, the site UT6 is located in the downstream area close to the Songkhla Lake, so a less steep channel slope is expected. This reduced slope would result in reduced boundary shear stress and, in turn, would reduce the fluvial erosion potential. At the other extreme, the

Table 3 Aerial imagery analysis results

Site	Distance from UT1 (m)	Land use	Reach length (m)	Bank retreat (m)		
				R_{2010}	R_{2016}	R_T
UT1	–	Rubber plantation	78.04	10.08	1.87	11.96
UT2	4973	Rubber plantation	69.69	9.39	11.14	20.52
UT3	5203	Rubber plantation	128.78	9.08	8.31	17.39
UT4	6333	Rubber plantation	74.83	6.59	7.44	14.04
UT5	7690	Rubber plantation	55.09	11.76	20.06	31.83
UT6	13,990	Village	78.37	3.04	4.48	7.52
			Average	8.33	8.88	17.21

highest bank retreat was found at the site UT5 with R_{2010} , R_{2016} , and R_T being 11.76, 20.06, and 31.83 m, respectively. The R_{2010} does not differ much from that of the other sites, but R_{2016} does. Aerial images of this site clearly show that during 2002 to 2010, retreat occurred but the bank remained straight. However, river bank concave in shape is observed in the 2016 aerial image. Concave banks generally cause both curvature-driven and turbulence-driven secondary flows that alter the flow fields and the morphology of the banks (Camporeale et al. 2007; Papanicolaou et al. 2007). These secondary flows are here considered to be the major cause of high R_{2016} of this site. The reason for the emergence of the concave shape at this site is not known. However, it is believed that soil heterogeneity in the river banks combined with the complexity of subaerial and hydrogeological processes to cause this.

At the site UT1, R_{2010} , R_{2016} , and R_T were 10.08, 1.87, and 11.96 m, respectively. R_{2016} was much less than R_{2010} or retreats at the other sites (Table 3). Course change of the U-

Tapao River was the cause of the low R_{2016} observed at this site. It is believed that a big flood in 2010 changed the course of the river, as observed in the aerial images, so that the site UT1 became located on the inside of a bend. Bank accretion and formation of point bars are usually found at the insides of bends (Motta et al. 2012).

Riverbank retreat analysis results

The bank retreats (R_{2010}) from BSTEM runs using the τ_c and k_d values from the jet tests were 0.0 m (no retreat) at the sites UT1, UT5, and UT6. In contrast, the R_{2010} values at sites UT2 to UT4 were very large exceeding 100 m. These simulation results differed dramatically from the observed R_{2010} values, measured from aerial images (Table 3). The incorrect R_{2010} estimates from BSTEM runs were caused by several factors. Among these were the spatial and temporal changes of fluvial resistance of the bank materials, due to wetting/drying cycles.

Table 4 Bank retreat analysis results compared to BSTEM simulation runs with adjusted erodibility parameters

Site	Bank layer	JET test		α	Adjusted values		R_{2010} (m)		R_{2016} (m)		R_T (m)	
		τ_c (Pa)	k_d (cm ³ /N.s)		τ_c (Pa)	k_d (cm ³ /N.s)	AIA	BSTEM	AIA	BSTEM	AIA	BSTEM
UT1	Upper	13.18	4.13	2.986	4.41	12.33	10.08	9.48	1.87	11.81	11.96	21.29
	Lower	14.37	3.67	2.986	4.81	10.95						
UT2	Upper	20.93	1.74	1.000	20.93	1.74	9.39	9.74	11.14	8.74	20.52	18.48
	Lower	1.43	19.55	0.290	4.77	5.86						
UT3	Upper	7.12	6.48	0.492	14.47	3.19	9.08	9.05	8.31	10.59	17.39	19.64
	Lower	2.41	11.36	0.492	4.89	5.59						
UT4	Upper	16.47	2.23	1.000	16.47	2.23	6.59	6.11	7.44	6.55	14.03	12.66
	Lower	2.68	7.98	0.474	5.65	3.78						
UT5	Upper	8.80	3.39	1.000	8.80	3.39	11.76	13.19	20.06	19.25	31.83	32.45
	Lower	16.88	6.55	3.162	5.34	20.70						
UT6	Upper	8.41	14.29	0.800	10.52	11.43	3.04	3.39	4.48	3.41	7.52	6.80
	Lower	16.56	15.07	2.653	6.24	39.99						
RMS (m)							0.69		4.32		4.06	

BSTEM, Bank Stability and Toe Erosion Model; AIA, aerial imagery analysis; τ_c , critical shear stress, k_d , erodibility coefficient; R_{2010} , bank retreat from 2002 to 2010, R_{2016} , bank retreat from 2010 to 2016, R_T , $R_{2010} + R_{2016}$; RMS, root mean square error between BSTEM and AIA retreats

Fluvial resistance is typically measured at a specific time, but due to the wetting/drying cycles and the subaerial processes, the observed τ_c and k_d can change considerably over time (Daly et al. 2015). Furthermore, the bank retreat can progress inland over a long time period so that it encounters spatial changes of the bank materials, and this affects the τ_c and k_d as well.

To improve the computed bank retreat results, the τ_c and k_d values were adjusted iteratively using trial lumped adjustment factors (α) in a series of BSTEM runs, until the computed R_{2010} were optimally close to the values measured from aerial imagery. The α , adjusted τ_c and k_d , and computed R_{2010} values are tabulated in Table 4. It was found that α values approximately from 0.3 to 3.0 were sufficient to adjust the τ_c and k_d so that the computed R_{2010} were in good agreement with the measured ones. For sites UT1 and UT3, use of equal α values for upper and lower banks provided good R_{2010} results. However, for sites UT2 and UT4 to UT6, it was found that the R_{2010} were caused only by erosion of the lower banks. Thus, for these sites, the calibration of α was conducted solely on the lower banks while the α values of the upper banks were kept as unity. The computed R_{2010} obtained from BSTEM runs for all sites considered were fairly similar to the observed values, as shown in Fig. 7: the points in the scatter plot fall close to the diagonal line with identical values. The computed and measured R_{2010} differed in terms of the root mean square (RMS) error by as low as 0.69 m (Table 4), showing that BSTEM with adjusted erodibility parameters can be used to accurately fit our data, modeling the appropriate failure mechanisms of fluvial toe erosion leading to bank undercutting and sloughing of upper cohesive layers, as commonly observed in composite riverbank studies (Rinaldi et al. 2008).

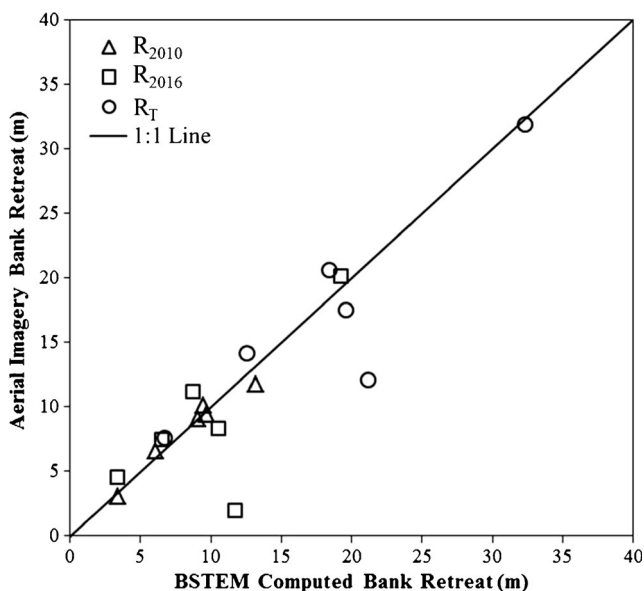


Fig. 7 Comparison of bank retreat measured from aerial imagery to bank retreat computed with BSTEM

Bank retreats (R_{2016}) calculated using BSTEM with the adjusted τ_c and k_d values, and another set of hydrographs from 2010 to 2016 are tabulated in Table 4. The R_{2016} values calculated using BSTEM compared well with the corresponding R_{2016} values measured from aerial imagery, for all sites except the site UT1. For the sites UT2 to UT6, the absolute difference between measured and computed R_{2016} ranged from 0.81 to 2.40 m with an average of 1.49 m. This indicates that the erodibility parameters obtained using the lumped adjustment factor could be effectively used to predict the bank retreat. The τ_c and k_d obtained using this technique are better than those obtained from empirical formulae or the jet tests, because these parameters already account for the “lumped” subaerial process, fluvial erosion, and slope failure.

For the site UT1, however, the computed R_{2016} overestimated the R_{2016} considerably, by +9.94 m (Table 4). As mentioned previously, the river course change observed at site UT1 was the probable reason to this overestimate. The R_{2016} computed using the adjusted erodibility parameters to model R_{2010} (the course change of the river had not yet occurred) should show about similar rate of retreat as R_{2010} , given that the hydrograph between these two periods was not much different. However, due to the river course change, turning this site to the inner bend bank, the actual retreat reduced or even reversed to bank accretion. The measured R_{2016} at this site that was much less than predicted using BSTEM is entirely reasonable on this basis.

Conclusions

Steep riverbanks of the U-Tapao River in southern Thailand consisted of two layers. The thickness of upper and lower banks varied from 1.0 to 1.5 m and 3.0 to 6.2 m, respectively. Toe erosion at the lower banks was observed to continuously lead to bank failure. Laboratory test results showed that the riverbank soils along the U-Tapao River consisted of silty sand, low plasticity silt, low plasticity clay, and high plasticity clay. The erodibility parameters from the jet tests indicated that the soils can be classified as erodible to very erodible which were very susceptible to erosion. In addition, the lower bank soils were found to be more erodible than the upper ones. Aerial imagery analysis results revealed that the observed bank retreat from 2002 to 2016 ranged from 7.52 to 31.83 m with an average of 17.21 m. Process-based riverbank retreat analysis which incorporates the erosion of the riverbank soil through excess shear stress equation and the riverbank failure through slope stability equation was conducted using the Bank Stability and Toe Erosion Model (BSTEM) to compute long-term riverbank retreat. The computed retreats were verified with the observed ones. Initial BSTEM runs using the erodibility parameters obtained either from the jet test or the empirical formula over the period from 2002 to 2010 did not

provide good predictions of bank retreat. However, good agreement of the retreats was achieved by adjusting the erodibility parameters iteratively, using the lumped adjustment factor. The adjusted critical shear stress and erodibility coefficient of the erodible riverbank soils ranged from 4.41 to 20.93 Pa and 2.23 to 39.99 cm³/N.s. These adjusted erodibility parameters are believed to account for local subaerial processes, fluvial erosion, and slope failures that cause the bank retreat. Another set of BSTEM runs using adjusted erodibility parameters was further validated against later observations, over the period from 2010 to 2016, and appeared to provide reasonably good predictions of river bank retreat.

Acknowledgements The authors would like to thank Dr. Seppo Karrila for reviewing the manuscript, Dr. Eddy Langendoen of the United States Department of Agriculture for providing BSTEM v. 5.4, and Dr. Garey Fox of Oklahoma State University for providing a JET spreadsheet for the jet test computations. Finally, the authors would like to thank anonymous reviewers for their helpful and constructive comments that greatly contributed to the improvement of the final version of the paper.

Funding information Financial support for this study was provided by the Prince of Songkhla University and the National Research Council of Thailand, grant no. ENG570109S. This support is gratefully acknowledged.

References

- Al-Madhhachi AT, Hanson GJ, Fox GA, Tyagi AK, Bulut R (2013) Deriving parameters of a fundamental detachment model for cohesive soils from flume and jet erosion tests. *T ASABE* 56(2):489–504
- ASCE Task Committee on Hydraulics, Bank Mechanics, and Modeling of River Width Adjustment (1998) River width adjustment: I processes and mechanisms. *J Hydraul Eng* 124(9):881–902
- Blaisdell FW, Anderson CL, Hebaus GG (1981) Ultimate dimensions of local scour. *J Hydraul Eng Div* 107(HY3):327–337
- Briaud JL, Ting FCK, Chen HC, Cao Y, Han SW, Kwak KW (2001) Erosion function apparatus for scour rate predictions. *J Geotech Geoenviron ASCE* 127(2):105–113
- Camporeale C, Perona P, Porporato A, Ridolfi L (2007) Hierarchy of models for meandering rivers and related morphodynamic processes. *Rev Geophys* 45:RG1001
- Cancienne RM, Fox GA, Simon A (2008) Influence of seepage undercutting on the stability of root-reinforced streambanks. *Earth Surf Proc Land* 33(1):1769–1786
- Clark LA, Wynn TM (2007) Methods for determining streambank critical shear stress and soil erodibility: implications for erosion rate predictions. *T ASABE* 50(1):95–106
- Couper PR, Maddock IP (2001) Subaerial river bank erosion processes and their interaction with other bank erosion mechanisms on the River Arrow, Warwickshire, UK. *Earth Surf Proc Land* 26:631–646
- Daly ER, Fox GA, Al-Madhhachi AT, Miller RB (2013) A scour depth approach for deriving erodibility parameters from jet erosion tests. *T ASABE* 56(6):1343–1351
- Daly ER, Miller RB, Fox GA (2015) Modeling streambank erosion and failure along protected and unprotected composite streambanks. *Adv Water Resour* 81:114–127
- Grissinger EH, Little WC, Murphey JB (1981) Erodibility of streambank materials of low cohesion. *T ASAE* 24(3):624–630
- Grissinger EH (1982) Bank erosion in cohesive materials. In: Hey RD, Bathurst JC, Thorne CR (eds) *Gravel-bed rivers*. John Wiley, pp. 273–287
- Grissinger EH, Bowie AJ, Murphey JB (1991) Goodwin Creek bank instability and sediment yield. *Proceeding of the 5th Federal Interagency Sedimentation Conference*, U. S. Government Printing Office, Washington, D.C, pp PS-32–PS-39
- Hanson GJ (1990a) Surface erodibility of earthen channels at high stresses: Part I. Open channel testing. *T ASABE* 33(1):127–131
- Hanson GJ (1990b) Surface erodibility of earthen channels at high stresses: Part II. Developing an in situ testing device. *T ASABE* 33(1):132–137
- Hanson GJ, Cook KR (1997) Development of excess shear stress parameters for circular jet testing. *ASAE Paper No. 972227*. ASAE, St. Joseph, Mich
- Hanson GJ, Cook KR, Simon A (1999) Determining erosion resistance of cohesive materials. *Proceedings of ASCE International Water Resources Engineering Conference*. Seattle, Wash, ASCE
- Hanson GJ, Simon A (2001) Erodibility of cohesive streambeds in the loess area of the Midwestern USA. *Hydrol Process* 15(1):23–38
- Hanson GJ, Temple DM (2002) Performance of bare-earth and vegetated steep channels under long-duration flows. *T ASAE* 45(3):695–701
- Hanson GJ, Cook KR (2004) Apparatus, test procedures, and analytical methods to measure soil erodibility in situ. *Appl Eng Agric* 20(4):455–462
- Hooke JM (1979) An analysis of the processes of riverbank erosion. *J Hydrol* 42:39–62
- Julian JP, Torres R (2006) Hydraulic erosion of cohesive riverbanks. *Geomorphology* 76(1–2):193–206
- Kamphuis JW, Hall KR (1983) Cohesive material erosion by unidirectional current. *J Hydraul Eng* 109(1):49–61
- Karmaker T, Dutta S (2011) Erodibility of fine soil from the composite river bank of Brahmaputra in India. *Hydrol Process* 25(1):104–111
- Langendoen EJ, Simon A, Alonso CV (2000) Modeling channel instabilities and mitigation strategies in Eastern Nebraska, *Proceeding of the 2000 Joint Conference on Water Resources Engineering and Water Resource Planning and Management*. ASCE, New York
- Langendoen EJ, Simon A (2008) Modeling the evolution of incised streams, II: streambank erosion. *J Hydraul Eng* 134(7):905–915
- Lai YG, Thomas RE, Ozeren Y, Simon A, Greimann BP, Wu K (2012) Coupling a two-dimensional model with a deterministic bank stability model. *ASCE World Environmental & Water Resources Congress*. Albuquerque, New Mexico May 20–24, 2012
- Lawler DM (1992) Process dominance in bank erosion systems. In: Carling PA, Petts GE (eds) *Lowland floodplain rivers, Geomorphological Perspectives*. John Wiley, pp. 117–143
- Lawler DM (1995) The impact of scale on the processes of channel-side sediment supply: a conceptual model. *Effects of scale on interpretation and management of sediment and water quality*. IAHS Pub 226: 175–184
- Lawler DM, Thorne CR, Hooke JM (1997) Bank erosion and instability. In: Thorne CR, Hey RD, Newson, MD (eds) *Applied Fluvial Geomorphology for River Engineering and Management*. John Wiley, pp. 137–172
- Midgley T, Fox GA, Heeren DM (2012) Evaluation of the bank stability and toe erosion model (BSTEM) for predicting lateral streambank retreat on composite streambanks. *Geomorphology* 145–146:107–114
- Motta D, Abad JD, Langendoen EJ, Garcia MH (2012) A simplified 2D model for meander migration with physically-based bank evolution. *Geomorphology* 163:10–25
- Nardi L, Campo L, Rinaldi M (2013) Quantification of riverbank erosion and application in risk analysis. *Nat Hazards* 69:869–887
- Papanicolaou AN, Elhakeem M, Hilldale R (2007) Secondary current effects on cohesive river bank erosion. *Water Resour Res* 43: W12418

- Partheniades E (1965) Erosion and deposition of cohesive soils. *J Hydraul Div* 91:105–139
- Rinaldi M, Mengoni B, Luppi L, Darby SE, Mosselman E (2008) Numerical simulation of hydrodynamics and bank erosion in a river bend. *Water Resour Res* 44(9):W09429
- Rinaldi M, Nardi L (2013) Modeling interactions between riverbank hydrology and mass failures. *J Hydraul Eng* 18(10):1231–1240
- Semmens DJ, Osterkamp WR (2001) Dam removal and reservoir erosion modeling: Zion Reservoir, Little Colorado River, AZ. Proceedings of the Seventh Federal Interagency Sedimentation Conference. March 25–29, 2001, Reno, NV, pp. IX 72–79
- Smerdon ET, Beasley RT (1961) Critical tractive forces in cohesive soils. *Agric Eng* 42(1):26–29
- Simon A (1989) A model of channel response in disturbed alluvial channels. *Earth Surf Proc Land* 14:11–26
- Simon A, Curini A, Darby SE, Langendoen EJ (2000) Bank and near-bank processes in an incised channel. *Geomorphology* 35:193–217
- Simon A, Thomas RE (2002) Processes and forms of an unstable system with resistant, cohesive streambeds. *Earth Surf Proc Land* 27(7): 699–718
- Simon A, Thomas RE, Klimetz L (2010) Comparison and experiences with field techniques to measure critical shear stress and erodibility of cohesive deposits. Proceedings of the 2nd Joint Federal Interagency Conference on Sedimentation and Hydrologic Modeling. Reston, Va, U.S. Geological Survey. ASTM, Philadelphia, Penn
- Simon A, Pollen-Bankhead N, Thomas RE (2011) Development and application of a deterministic bank stability and toe erosion model for stream restoration. In *Stream Restoration in Dynamic Fluvial Systems: Scientific Approaches, Analyses, and Tools*, 453–474, Geophysical Monograph Series, vol vol. 194. American Geophysical Union, Washington, D.C
- Thoman RW, Niezgoda SL (2008) Determining erodibility, critical shear stress, and allowable discharge estimates for cohesive channels: case study in the Powder River basin of Wyoming. *J Hydraul Eng* 134(12):1677–1687
- Thorne CR (1982) Processes and mechanisms of river bank erosion. In: Hey RD, Bathurst JC, Thorne CR (eds) *Gravel-bed rivers*. John Wiley, pp. 227–271
- Wan CF, Fell R (2004) Investigation of rate of erosion of soils in embankment dams. *J Geotech Geoenviron* 130(4):373–380
- Wilson GV, Periketi R, Fox GA, Dabney S, Shields D, Cullum RF (2007) Seepage erosion properties contributing to streambank failure. *Earth Surf Proc Land* 32(3):447–459
- Wynn T (2004) The effects of vegetation on streambank erosion. Dissertation, Department of Biological Systems Engineering, Virginia Tech
- Wynn TM, Mostaghimi S (2006) Effects of riparian vegetation on stream bank subaerial processes in southwestern Virginia, USA. *Earth Surf Pro Land* 31:399–413